RSC Advances

PAPER

View Article Online
View Journal | View Issue

Cite this: *RSC Adv.*, 2024, **14**, 36398

Research on the underground gasification of lignite through an oxygen enrichment process: insights from experimental study and Aspen Plus process model

Jishuang Ding,[a] Caifang Wu,[bc] Bin Gao,[*d] Shengxu Zhang,[a] Jinbiao Zhang[a] and Kaiyue Tan[a]

Underground coal gasification (UCG) can convert coal resources to high-calorific value syngas, which is important for the exploration of resources and the application of clean coal technology. This study investigated the gasification process of lignite in Heilongjiang Province through an oxygen enrichment approach and examined the impact of the oxygen concentration on the gasification efficiency. Furthermore, a high-fidelity Aspen Plus process model was designed to predict the gasification products of lignite. These findings indicate that the abrupt increase in the gasification temperature and pressure is governed by the concentration of oxygen in the gasification agent. An increased concentration of oxygen results in a higher gasification temperature, thereby influencing the thermodynamic reaction processes within the gasifier. The combustion reaction of lignite transitions into a coke reaction when the oxygen concentration is elevated to 90%. At this time, the relative concentration of CO_2 generated from lignite combustion progressively diminished from 78.33%, while the relative concentrations of H_2 and CO produced through coke reactions gradually increased from 3% and 2.07%, respectively. When the oxygen concentration reaches 100%, the relative contents of H_2 and CO generated through gasification reach their respective maxima, measuring 18.90% and 23.91%. The calorific value attained a peak of 6.65 MJ N^{-1} m^{-3} simultaneously. Furthermore, the ash yield of lignite may be a critical factor influencing the process of underground coal gasification. The gasification efficiency of lignite near T_6 is suboptimal when the oxygen concentration falls below 100%, potentially attributable to the influence of ash. In summary, lignite in Heilongjiang Province can be effectively developed through underground gasification technology *via* an oxygen enrichment process. Furthermore, the Aspen Plus model we developed can effectively assist in predicting the products of lignite gasification in Heilongjiang Province.

Received 14th September 2024
Accepted 11th November 2024

DOI: 10.1039/d4ra06654e

rsc.li/rsc-advances

1. Introduction

Lignite accounts for 18% of the total global coal reserves and is an important energy supply.[1] The coal resources of Heilongjiang Province, China, are rich, accounting for 36.06% of the province's coal. Lignite is typically distinguished by its elevated moisture content and relatively low calorific value.[2,3] Moreover, spontaneous combustion can easily occur, which greatly increases the cost of transportation and storage. Furthermore, certain sections of the lignite coal-bearing strata in Heilongjiang Province exhibit semicemented diagenesis, resulting in relatively weak rock formations. In contrast, the roofs of some coal seams consist of siltstone, whereas the base is composed of mudstone, providing excellent structural support. However, these formations are constrained by the conditions associated with open-pit and underground mining. Clearly, a new strategy for lignite development is urgently needed. Underground coal gasification (UCG) is a technology for the *in situ* controlled combustion of coal that can directly convert coal into combustible gases (H_2, CO, CH_4, *etc.*) underground.[1,4–9] It is considered to be an effective method for recovering deep coal resources, thin coal seams that are difficult to mine *via* conventional underground methods, and discarding coal resources in abandoned mines.[10–12] This technology reduces the environmental damage caused by coal combustion, has good environmental benefits, and can promote the clean utilization of coal.[13–18] Consequently, in light of the stability constraints of the surrounding rock during the gasification process, it is crucial to investigate underground gasification methods for

[a]*Natural Resources Survey Institute of Heilongjiang Province, Harbin 150036, China*
[b]*Key Laboratory of Coalbed Methane Resource & Reservoir Formation Process, Ministry of Education, China University of Mining & Technology, Xuzhou 221116, China*
[c]*School of Resources and Earth Science, China University of Mining & Technology, Xuzhou 221116, China*
[d]*School of Construction Management, Jiangsu Vocational Institute of Architectural Technology, Xuzhou 221116, China. E-mail: gaobin_gms@163.com*

extracting lignite from stable coal-bearing strata rather than from softer coal-bearing strata in Heilongjiang Province, as this approach significantly enhances resource utilization.

Scholars have experimentally studied the influence of gasification technology on gas production and temperature in the UCG process. It is generally believed that the type of gasification product depends on the thermodynamic conditions of the gasification process and the composition of the gasification agent used.[17,19,20] Gasification media such as air, oxygen, and/or steam are used in gasification engineering.[21,22] Different gasification agents correspond to different gasification processes, but the reactions between coal and gasification media are essentially the same in the gasification process.[15,23,24] The calorific value obtained with oxygen as the gasification agent is generally 1 MJ N^{-1} m^{-3} higher than that of other gasification agents.[1,2,25] Oxygen and air are widely used gasification agents, but the applicable scenarios of steam need to be selected according to the coal type.[25,26] Moreover, in previous studies, inert process conditions were established by adding nitrogen to gasification agents, which were subsequently used to cool the reactor after the gasification experiment was completed.[5] Importantly, while the gasification agent significantly influences the gasification products, the intrinsic properties of the coal being gasified must not be overlooked. Several studies have indicated that the efficiency of gasification diminishes as the ash yield in coal increases.[6,27,28] Furthermore, the impact of pressure on gasification products, particularly methane, is markedly significant throughout the gasification process.[29] It is evident that the gasification efficiency is influenced by either the gasification environment or the characteristics of the coal itself, presenting a significant issue for further consideration.

In the study of underground coal gasification products, the Aspen Plus model can be employed to predict the composition of syngas generated from underground coal gasification, in addition to the use of physical simulation devices for conducting gasification experiments. Aspen Plus is a globally recognized process for steady-state chemical simulation software that is based on process technology. A process simulation system can be used to visualize the thermal reaction process of coal gasification in a gasifier. Notably, the gas components produced during coal gasification are controlled by various chemical reactions in the gasifier.[30,31] Thus, Aspen Plus software can be used to assist in the study of the entire coal gasification process.[32] Scholars frequently employ the thermal balance method for modelling, which assumes that the coal gasification process and its associated chemical reactions achieve thermodynamic equilibrium. By applying the principle of minimum equilibrium energy, this approach predicts the composition, yield, and temperature of the produced gas.[33] Many underground coal gasification models have been constructed under this assumption to predict the perinational process. The LVW and CRIP models, which are two very important theoretical models, are worth mentioning.[31,33] However, the Aspen plus process is relatively complex, and many scholars only rely on coal pyrolysis experiments for design, which is obviously not enough and will lead to ideal simulation results. Thus, it is very important to design an Aspen Plus gasification process that is based on coal pyrolysis data and uses underground coal gasification physical simulation experimental data as calibration samples to achieve accurate prediction of underground coal gasification. Nevertheless, constructing Aspen Plus process models that align with physical simulation experiments to achieve consistent gasification results remains a formidable challenge.

Lignite is considered to be a low-value coal and is abundant in reserves.[3,34] Therefore, its exploration and utilization have attracted much attention from scholars.[1,3,35] The evaporation of water during the gasification of lignite leads to significant heat loss, which consequently results in a low calorific value of the generated gas.[1,2,25] However, the yield of H_2 can be greatly increased by using steam as the gasification agent when there is less water in the coal.[4] Previous studies have confirmed the feasibility of developing lignite coal seams *via* underground gasification technology.[1,34] The calorific values of gas produced by lignite from Slovenia and Romania are 6.4 MJ N^{-1} m^{-3} and 4.8 MJ N^{-1} m^{-3}, respectively.[34]

On the basis of the above analysis, this study used lignite from the Chaoyang open-cast coal mine in Heilongjiang Province for underground gasification experiments. The Aspen Plus process model was developed on the basis of physical simulation experiments and pyrolysis data. The gasification characteristics of lignite were investigated *via* an oxygen-enriched process. The variation trend of the gas product relative concentration under different oxygen concentration conditions was elucidated, and the primary controlling factors influencing lignite underground gasification were revealed. Moreover, the present study offers an optimal O_2 concentration ratio scheme for a gasification project in Heilongjiang Province, ensuring the most effective gasification agent utilization. Furthermore, the Aspen Plus process model developed in this study is capable of predicting lignite gasification products specific to Heilongjiang Province, thereby offering a novel approach for the exploration and utilization of lignite resources in the region.

2. Experimental methodology

2.1 Materials

The gasification coal used in this study was collected from the Chaoyang open-cast coal mine in Heilongjiang Province. The maximum reflectance of vitrinite ($R_{o,max}$), proximate analysis, and ultimate analysis information of the samples are shown in Table 1. A fixed bed cutting machine was used to cut the sample 0.3 × 0.3 × 0.2 m along the bedding direction for the underground gasification physical simulation experiments. Fig. 1 shows the state of the sample after being placed on the underground gasification simulation platform.

2.2 Experimental apparatus and process

2.2.1 Physical simulation experimental apparatus. A schematic of the physical simulation experimental apparatus is shown in Fig. 1. It is mainly composed of a simulated gasifier, a gasification agent supply system, a syngas cooling system, a tar separation system, and a thermal coupling temperature

Table 1 $R_{o,max}$, proximate, and ultimate analysis information of gasified lignite

	Proximate analysis (%)				Ultimate analysis (%)					
$R_{o,max}$%	M_{ad}	A_{ad}	V_{ad}	FC_{ad}	C_{daf}	H_{daf}	O_{daf}	N_{daf}	S_{daf}	Cl_{daf}
0.42	9.68	26.43	66.50	33.50	60.58	6.37	31.52	0.56	0.91	0.06

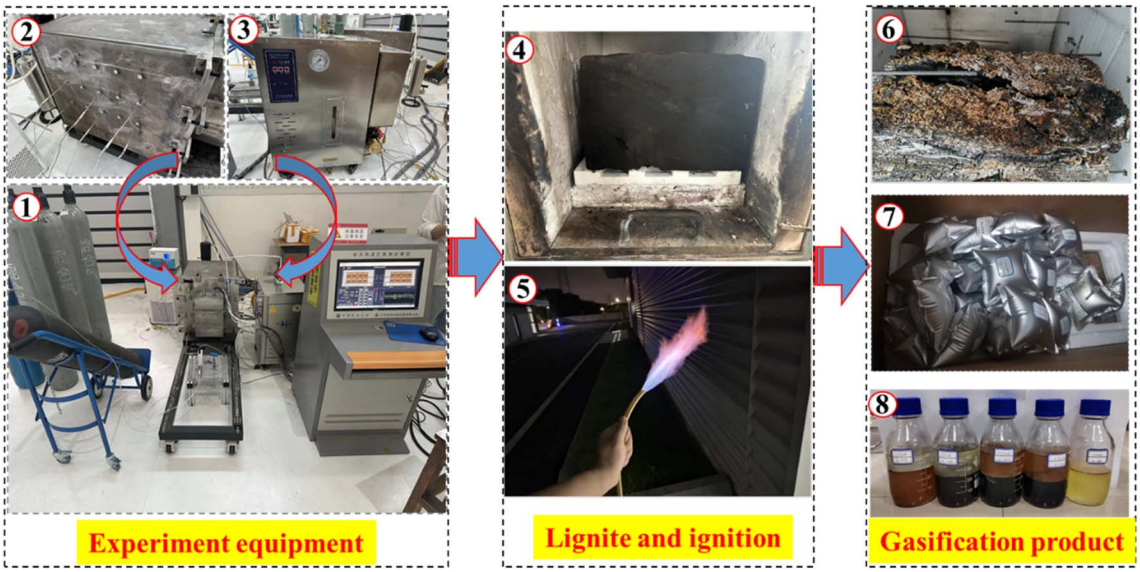

Fig. 1 Experimental apparatus and physical simulation experimental process of lignite underground gasification ((1) the physical simulation apparatus for underground lignite gasification; (2) gasifier; (3) electric simulation steam generator; (4) gasified lignite; (5) syngas firing; (6) char; (7) syngas; (8) Tar).

detection panel. The space in the gasifier is rectangular, and its size is approximately 0.3 m × 0.3 m × 0.4 m. There are 15 thermal coupling device holes on both sides of the furnace body, which are connected to the thermal coupling device to monitor the reaction temperature. The gasification agent supply system is mainly composed of external gas tanks. Air, O_2, N_2, CO_2, and water vapour can be used as gasification agents. The steam is provided mainly by the electric steam generator. Furthermore, the apparatus is outfitted with valves designed to periodically collect syngas and tar. Syngas can be measured by gas chromatography, and the main gas components, such as H_2, CH_4, CO, CO_2, and N_2, can be determined.[25]

Fig. 2 shows a schematic of the gasifier, while Fig. 3 shows the position of the ignition point both before and after the gasification experiment. Prior to the experiment, the coal underwent treatment, and six cavities approximately 10 cm in length (number 2 in Fig. 2) were drilled into the coal for the placement of temperature thermocouples (number 1 in Fig. 2). In this experiment, six temperature sensing devices were installed on both sides of the gasifier to monitor the temperature changes in the furnace in real time (Fig. 2). The temperature measuring devices on the left side are named T_2, T_3, T_5, and T_6, and those on the right side are named T_{11} and T_{13}. Notably, T_2 and T_3 are close to the ignition point (Fig. 3). Accordingly, the lignite here starts gasification earlier. In addition, the lignite at T_2 and T_3 is first in contact with the gasification agent, and its gasification reaction changes due to the concentration of different oxygen concentrations. The thermal response of T_2 and T_3 is more sensitive than that of the other temperature measurement devices.

Fig. 2 shows the heating apparatus (number 4 of Fig. 2) alongside the temperature sensing device (number 3 of Fig. 2). The operating temperature range of the heating device is between 100 °C and 1000 °C. The heating apparatus is connected to the coal at the ignition point, with the objective of igniting this point and facilitating the heating of the block coal within the gasifier until it reaches the combustion temperature. The gasification agent inlet is positioned at the front of the gasifier (number 6 in Fig. 2). The high-temperature gasification products generated during the experiment are directed into the condensing unit (number 5 of Fig. 2) located at the rear of the gasifier. The condensed product is directed into the gas storage tank for subsequent separation. The tar generated from the gasification process is collected *via* a mixture of carbon tetrachloride (CCl_4) and methanol (CH_3OH) at the exhaust port of the gas storage tank.

2.2.2 Physical simulation experimental process. The physical simulation experiment can be broadly categorized into three stages: the preparation phase, the execution phase, and the observation and sampling phase. In the preparation phase,

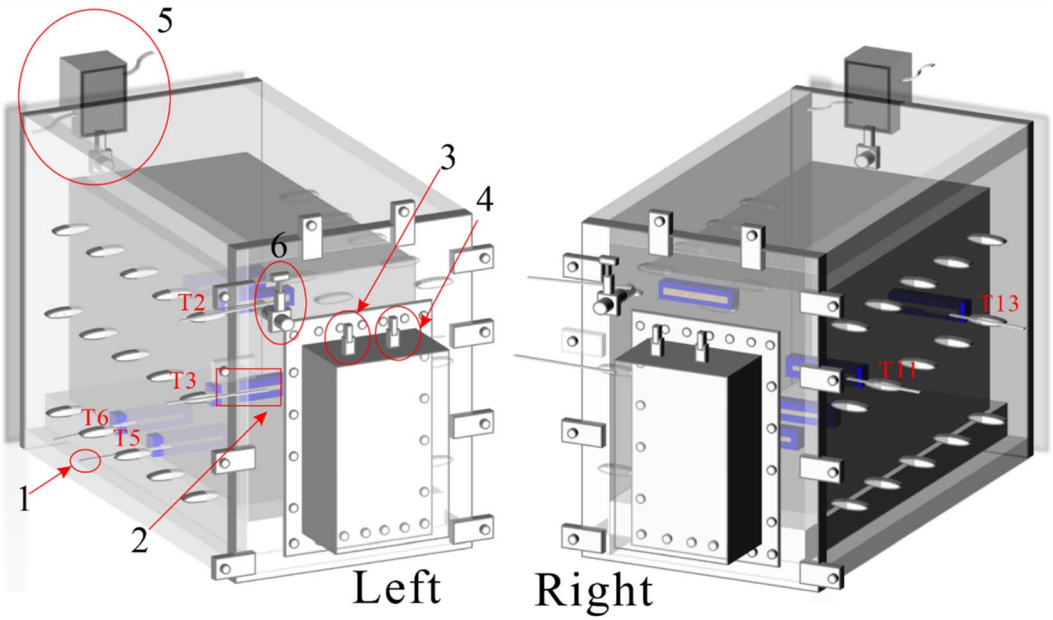

Fig. 2 Schematic representation of the simulated gasifier ((1) temperature sensing devices; (2) hollow cavity; (3) monitoring ignition point temperature device; (4) heating apparatus; (5) condensation apparatus; (6) inlet device for the gasification agent).

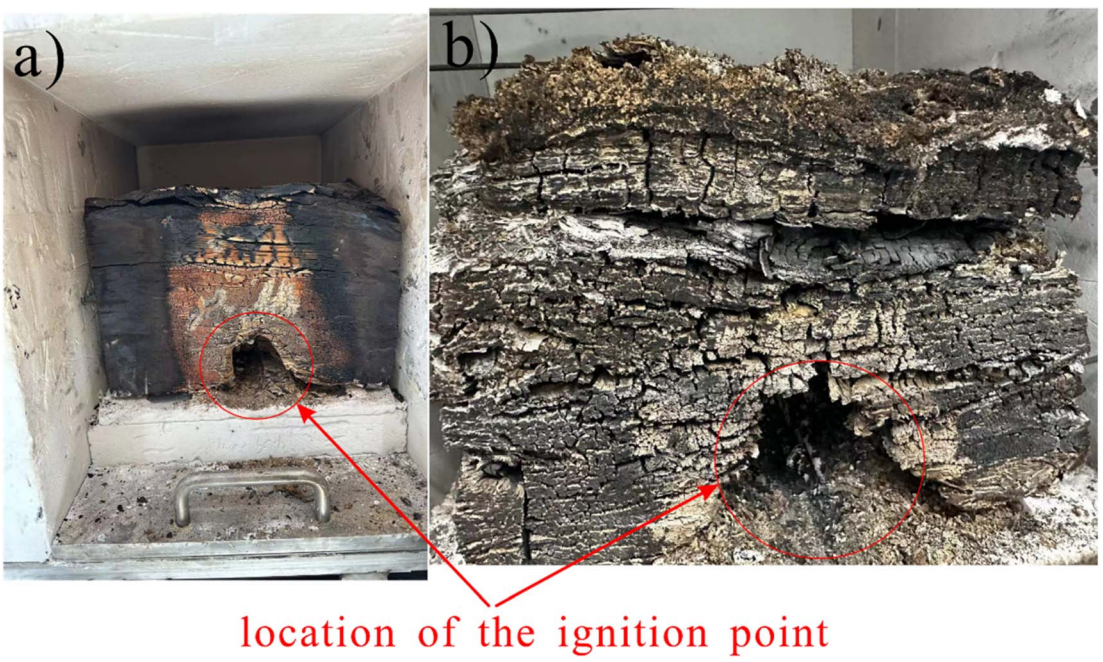

Fig. 3 Position of the ignition point (a) denotes the state of lump coal prior to the gasification reaction; (b) signifies its form subsequent to the gasification process.

five kinds of gasification agents were prepared according to the ratio of oxygen to nitrogen, which were 60% O_2–40% N_2, 70% O_2–30% N_2, 80% O_2–20% N_2, 90% O_2–10% N_2, and 100% O_2. This type of gasification agent has been proven to be applicable to underground gasification experiments on lignite.[1] A cavity approximately 30 cm in length is subsequently drilled into the base of the coal sample (Fig. 3) to function as a channel for coal gasification and to facilitate the connection of the ignition device. The simulated gasifier subsequently undergoes a cleaning process, followed by the sequential completion of loading, wiring, and sealing tasks.

In the execution phase, the five gasification agents are injected into the gasifier in turn according to the order of the oxygen concentration from 60% to 100% for each 120 minutes.

The flow rate of the gasification agent was 30 mL min^{-1}. The observation and sampling phases, upon completion of the ignition process, assess the success of ignition by monitoring the temperature variation at T_2. Once the temperature stabilized, gas and tar collection was conducted every 20 minutes. The cumulative collection duration of the gasification products was 10 hours. The temperature and pressure in the gasifier can reach 1000 °C and 0.45 MPa, respectively, when the gasification process is severe. Therefore, this study reduces the reaction efficiency by injecting water vapour into the gasifier to reduce the experimental risk.

2.3 Underground coal gasification balance model

In this study, a thermogravimeter was used to perform slow pyrolysis on the collected lignite samples, and a mass spectrometer was used to test the main components of pyrolysis gas. The experimental results can be used to clarify the pyrolysis characteristics of Cenozoic lignite in eastern Heilongjiang Province and provide a basis for the modelling of Aspen Plus software.

2.3.1 Lignite pyrolysis experiment. After the coal sample was loaded, high-purity nitrogen was injected into the reactor for 5 min, after which the temperature was raised from 27 °C to 900 °C at a heating rate of 10 °C min^{-1}. When the temperature reached 250 °C, 350 °C, 450 °C, 550 °C, 650 °C, 750 °C, 850 °C, and 900 °C, the produced gas was collected and tested. The composition of the produced gas was analysed. The results are shown in Table 2.

2.3.2 Aspen Plus process model. The pyrolysis process of lignite is consistent with the formation process of char. Therefore, the Aspen Plus process model can be designed on the basis of the pyrolysis data of lignite at different temperatures. As mentioned above, the Aspen Plus process model is designed according to certain rules and assumptions. The design principles of this process model refer to previous studies.[36–38] The process model designed in this study is shown in Fig. 4. The functions and applications of each operational unit in the process flow model are illustrated in Table 3.

The entire process flow model is divided into five regions, as depicted in Fig. 4, representing the different stages of the gasification process. These stages include wet coal drying (Stage 1), lignite oxidation (Stage 2), reduction (Stage 3), dry distillation zone formation (Stage 4), and component separation (Stage 5). The alignment between the physical simulation experiments and Aspen Plus simulations is demonstrated through three key aspects. Firstly, the model parameters are determined based on proximate analysis, ultimate analysis, and pyrolysis data while the process parameters are adjusted according to the results of physical simulation experiments, as detailed in the Section 3. Secondly, the Aspen Plus process model uses a rich oxygenation process for simulation experiments, which is consistent with the physical simulation experiments. The ratio between the coal intake and the gasification agent flow was determined by combining it with a physical simulation experiment. Specifically, when a coal intake of 60 kg h^{-1} is simulated, the initial gasification agent flow rate is 180 m^3 h^{-1}. Third, the consistency

Table 2 Pyrolysis composition and content of lignite at different temperatures

Temperature (°C)	Pyrolysis water (%)	Pyrolysis gas (%)	Tar oil (%)	Char (%)	Composition of pyrolysis gas (mL g^{-1})				
					CO_2	C_2–C_4	CO	CH_4	H_2
250	3.62	2.05	0.104	94.23	1.06	0.18	0.23	0.23	0.25
350	6.51	3.92	0.128	89.44	3.02	0.35	0.48	0.48	0.39
450	7.42	10.23	0.153	82.20	10.56	0.31	0.98	0.81	0.91
550	9.32	15.32	2.1	73.26	20.14	1.56	5.60	2.50	2.60
650	11.21	18.27	5.68	64.84	35.00	3.50	9.40	4.50	4.20
750	10.51	22.06	7.47	59.96	40.14	5.41	12.22	6.54	10.50
850	10.20	23.51	10.26	56.03	38.10	7.50	16.20	8.45	15.60
900	10.95	26.06	12.68	50.31	35.15	8.50	19.58	12.54	21.65

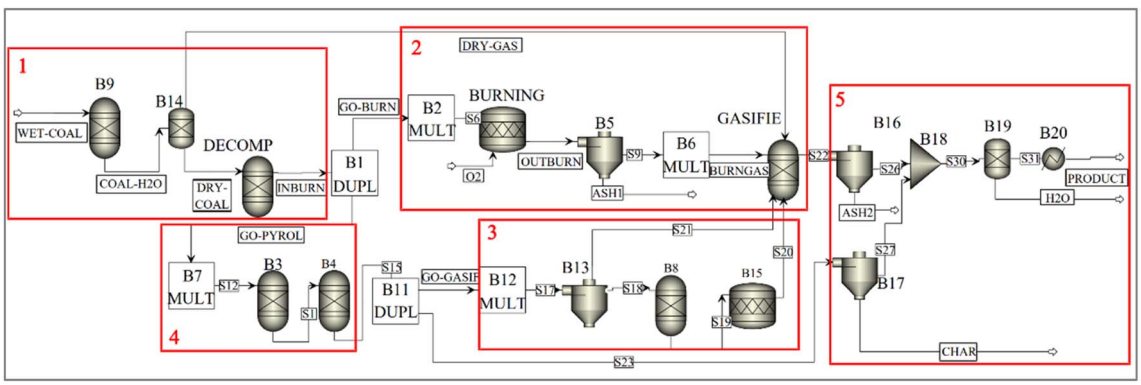

Fig. 4 Underground coal gasification model based on Aspen Plus software.

Table 3 Modules and functions of each operational unit in the gasification model

Operational unit	Modules	Functions
B9	RYield	Dried sample
B14, B19	SEP	Gas–solid–liquid separation
DECOMP	RYield	Coal is transformed into elemental form
BURNING	RStoic	Coal combustion
B5, B13, B16, B17	SSplit	Stream separation
GASIFIE	RGibbs	Gasification
B3, B4, B8	RYield	Thermal decomposition of coal and methanation reaction
B18	Mixer	Merging flow streams
B20	Heater	Cooling the gasified products

of the relative contents of different gasification products with respect to the oxygen concentration is important. The variation trends of each gasification product illustrated in Fig. 6 and 7 provide compelling evidence for this phenomenon. Both of these results are consistent with the trend of the relative concentration change in the gas products. Consequently, there is a high level of consistency between the gas production from the physical simulation experiment and that predicted by the Aspen Plus process flow model, thus confirming the strong rationality of the constructed process flow model in this study.

The oxygen concentration in the gasification agent can be manipulated as a variable in the Aspen Plus process model simulation to predict the composition and yield of the gasification product, thereby facilitating an analysis of the impact of the oxygen concentration on the resulting gasification product.

3. Results and discussion

3.1 Gasification process characteristics with respect to temperature

In this study, the combustion process of gasification agents is defined in five stages. The temperature information monitored by the six temperature measuring devices in the five gasification stages is shown in Table 4, including the initial, final, and average temperatures of each stage. The temperature change curve of each stage is shown in Fig. 5.

In the first stage, the initial and final temperatures of T_2, 3, 5, 6, 11, and 13 are 121.57–404.95 °C, 119.20–375.73 °C, 32.83–93.93 °C, 31.75–65.20 °C, 38.62–84.97 °C, and 42.97–88.84 °C, respectively. These average temperatures are 227.17 °C, 247.99 °C, 59.96 °C, 46.20 °C, 61.66 °C, and 63.32 °C, respectively. The temperature increases linearly with increasing combustion time on the basis of changes in the above temperature points. T_2 and T_3 are close to the ignition point; hence, their initial temperature is much higher than that of other temperature measuring devices. The temperatures of T_5, T_6, T_{11}, and T_{13} increase slowly, indicating that the combustion area is mainly concentrated at the front end during the initial combustion.

In the second stage, the initial and final temperatures of T_2, 3, 5, 6, 11, and 13 are 326.66–658.86 °C, 312.49–593.10 °C, 94.58–161.20 °C, 65.57–101.43 °C, 86.20–126.81 °C, and 89.37–132.90 °C, respectively. These average temperatures are 554.99 °C, 519.10 °C, 119.70 °C, 117.20 °C, 105.64 °C, and 119.73 °C, respectively. The temperature increased compared with that in the previous stage. The temperature changes in T_2 and T_3 are more obvious. Notably, between the first and second stages, there are obvious temperature fluctuations in the area near the ignition point (T_2 and T_3). This phenomenon is attributed to the replacement of the gasification agent between different gasification stages. This may represent a domain in which advancements are required for physics simulations. Perhaps an independent experiment for each oxygen concentration would yield better results. Nevertheless, given the brief duration of the replacement time, it can be inferred that its influence on the gasification process is minimal.

In the third stage, the initial and final temperatures of T_2, 3, 5, 6, 11, and 13 are 552.60–796.49 °C, 518.23–744.10 °C, 16.75–559 °C, 101.76–131.30 °C, 114.31–311.02 °C, and 131.51–369.06 °C, respectively. These average temperatures are 748.83 °C, 689.88 °C, 347.75 °C, 117.2 °C, 179.74 °C, and 234.52 °C, respectively. Compared with those in the first two stages, the temperatures of T_5, T_{11}, and T_{13} increased exponentially. This indicates that the combustion area began to extend backwards. Notably, the temperature of T_6 increases slowly, which indicates that the combustion on both sides of the gasifier is not uniform. The left combustion area extends slowly backwards.

In the fourth stage, the initial and final temperatures of T_2, 3, 5, 6, 11, and 13 are 690.47–971.72 °C, 678.18–915 °C, 550.20–

Table 4 Measured temperatures in the five gasification stages

	Temperature (°C)					
Stage	T_2	T_3	T_5	T_6	T_{11}	T_{13}
I	121.57–404.95	119.20–375.73	32.83–93.93	31.75–65.20	38.62–84.97	42.97–88.84
	277.17	247.99	59.96	46.20	61.66	62.32
II	326.66–658.86	312.49–593.10	94.58–161.20	65.57–101.43	86.20–126.81	89.37–132.90
	554.99	519.10	119.37	83.75	105.64	119.73
III	552.60–796.49	518.23–744.10	160.75–559	101.76–131.30	114.31–311.02	131.51–369.06
	748.83	689.88	347.75	117.20	179.74	234.52
IV	690.47–971.72	678.18–915	550.20–681.90	131.55–144.50	315.57–670.25	369.53–664.30
	892.44	851.74	605.15	139.25	526.74	559.67
V	798.23–1100.20	793.46–1076	669–927.31	121.06–607.30	660.89–906.13	648–868.28
	992.04	986.20	791.97	254.73	771.35	733.99

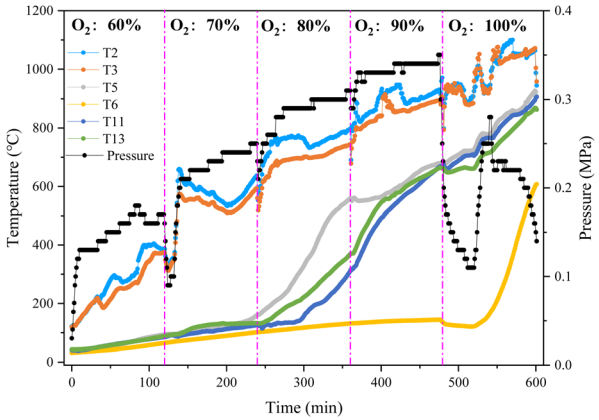

Fig. 5 Temperature and pressure variation curves of each temperature and pressure measurement device during gasification.

681.90 °C, 131.55–144.50 °C, 315.57–670.25 °C, and 369.53–664.30 °C, respectively. These average temperatures are 892.44 °C, 851.74 °C, 605.15 °C, 139.25 °C, 526.74 °C, and 559.67 °C, respectively. The higher temperature area of this stage further extends backwards, and the temperature distribution is more uniform than that of the previous stage. However, the lignite on the left side of the gasifier burns slowly backwards, and the temperature fluctuation at T_6 is relatively small.

In the fifth stage, the initial and final temperatures of T_2, 3, 5, 6, 11, and 13 are 798.23–1100.20 °C, 793.46–1076 °C, 669–927.31 °C, 121.06–607.30 °C, 660.89–906.13 °C, and 648–868.28 °C, respectively. These average temperatures are 992.04 °C, 986.20 °C, 791.97 °C, 254.73 °C, 771.35 °C, and 733.99 °C, respectively. The temperature of each temperature measurement device gradually increase, and the temperature of T_6 increases exponentially as well. This indicates that with increasing oxygen concentration in the gasification agent, the gasification process gradually intensifies. Moreover, the gasification area extends deeper backwards. In addition, at the end of the experiment, the temperature of each temperature measurement device still maintained an increasing trend, indicating that an increase in the oxygen concentration in the gasification agent increased the intensity of the gasification reaction.

3.2 Gasification process characteristics of pressure

The pressure change curve of underground lignite gasification in the gasifier during the simulation process is shown in Fig. 5. The pressure curve shows a downwards trend during the transition time of the five stages, that is, the time period of replacing the gasification agent. The fluctuation trend of the temperature curve is consistent with that of the pressure curve in the first four stages. These findings indicate that the temperature and pressure conditions of the gasifier clearly respond to a short period of gasification agent replacement. As the temperature increases, the pressure also increases in the first four stages, which means that the temperature in the gasifier is closely related to the pressure. This means that the gas production capacity is increasing. The pressure sensor setting of the simulation device was adjusted to ensure the safety of the experiment at the end of the fourth stage and the fifth stage. This directly led to the pressure drop of the gasifier, but it still showed the same pressure change trend as the first three stages did. Previous studies have shown that increasing pressure can improve the efficiency of the gasification process.[1,24,29] Zagorščak *et al.* demonstrated that under high-pressure gasification conditions, the total energy efficiency improved by 6%.[29] The relative content of effective gas components (H_2 and CO) obviously improved when combined with the analysis in Section 3.3.

3.3 Gasification process characteristics of the output syngas

3.3.1 Physical simulation experiment. A gas chromatography analyser (GC-950) was used to detect the components of the collected syngas to analyse the gas production capacity. The test time of each syngas was approximately 28 min. H_2, N_2, CO, CH_4, and CO_2 appeared successively on the spectrum, and the corresponding times were approximately 2 min, 4 min, 5.5 min, 12 min, and 22 min, respectively. Table 5 shows the results of the gas chromatography experiments. The minimum, maximum, and average relative content and calorific value of each gasification product are included in five stages. The changes in the concentration of the output syngas and calorific value during the process of underground coal gasification are shown in Fig. 6.

In the first stage, the relative content of H_2 was between 2.64% and 12.68%, with an average of 6.84%. The relative content of N_2 was between 35.31% and 59.26%, with an average of 47.09%. The relative content of CO was between 3.21% and 10.33%, with an average of 5.43%. The relative content of CH_4 was between 0.54% and 1.83%, with an average of 1.15%. The relative content of CO_2 was between 32.02% and 42.17%, with an average of 39.48%. The syngas component is mainly N_2, which is attributed to the high N_2 content in the gasification agent. The gas produced by lignite gasification is mainly CO_2, followed by H_2, CO, and CH_4 in this stage. The calorific value of the gas produced in this stage is between 1.96 MJ N^{-1} m^{-3} and 3.65 MJ N^{-1} m^{-3}, with an average of 2.02 MJ N^{-1} m^{-3}. The relative content of H_2 in this stage is relatively high, which may be related to the inherent moisture gasification in lignite. This phenomenon was consistent with the work of Zagorščak *et al.*[29]

In the second stage, the relative content of H_2 was between 0.48% and 1.19%, with an average of 0.73%. The relative content of N_2 was between 41.37% and 49.59%, with an average of 46.78%. The relative content of CO was between 2.07% and 3.98%, with an average of 3.98%. The relative content of CH_4 was between 0.24% and 0.42%, with an average of 0.31%. The relative content of CO_2 was between 45.58% and 54.58%, with an average of 48.99%. The relative content of N_2 was lower than that of CO_2 in this stage. The syngas is still dominated by N_2 and CO_2, followed by CO, H_2 and CH_4. The average calorific value of gas production in this stage is 0.62 MJ N^{-1} m^{-3}, which is lower than that in the first stage.

In the third stage, the relative content of H_2 was between 0.71% and 1.47%, with an average of 1.15%. The relative content of N_2 was between 25.75% and 27.36%, with an average

Table 5 Relative contents and calorific values of various output gases in the five gasification stages

oxygen concentration	H_2 (%)	N_2 (%)	CO (%)	CH_4 (%)	CO_2 (%)	Calorific value (MJ N^{-1} m^{-3})
60%	2.64–12.68	35.32–59.26	3.21–10.33	0.54–1.83	32.02–45.38	0.96–3.65
	6.84	47.09	5.43	1.15	39.48	2.02
70%	0.48–1.19	41.37–49.59	2.07–3.98	0.24–0.42	45.58–54.58	0.42–0.82
	0.73	46.78	3.19	0.31	49	0.62
80%	0.71–1.47	25.75–27.36	1.11–3.05	0.28–0.82	67.61–71.06	0.34–0.90
	1.15	26.62	1.83	0.50	69.91	0.58
90%	3–14.90	9.80–15.61	2.07–8.53	0.75–2.03	64.73–78.33	0.94–3.79
	6.33	13.87	4.10	1.13	74.57	1.77
100%	16.37–18.90	1.37–2.46	8.75–23.91	0.50–3.06	55.51–70.85	3.39–6.65
	17.89	1.78	17.88	1.46	61.10	5.12

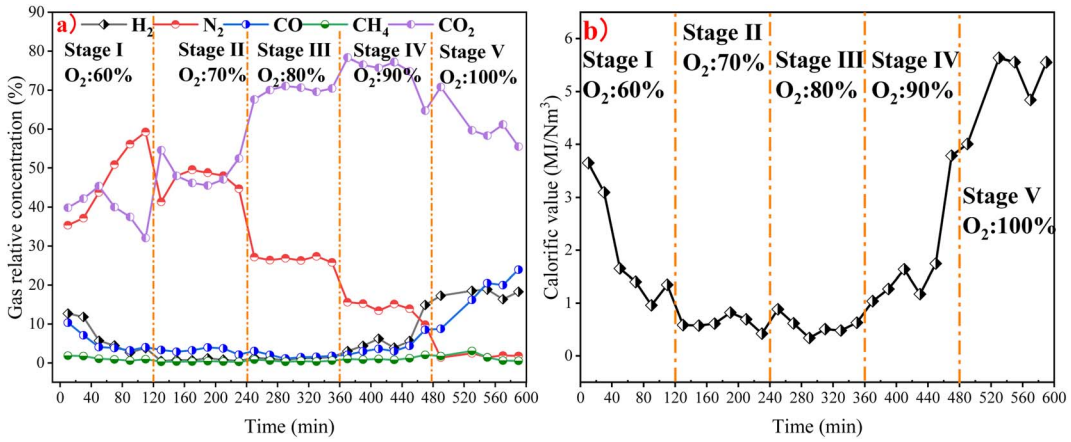

Fig. 6 Characteristics of the syngas and calorific value in the underground coal gasification experiment: (a) characteristics of the syngas, (b) characteristics of calorific value.

of 26.62%. The relative content of CO was between 1.11% and 3.05%, with an average of 1.83%. The relative content of CH_4 was between 0.28% and 0.82%, with an average of 0.50%. The relative content of CO_2 was between 67.61% and 71.06%, with an average of 69.91%. The gas composition is still dominated by CO_2, followed by N_2 at this stage. However, the relative contents of H_2, CO, and CH_4 are low. The average calorific value of gas production in this stage is 0.58 MJ N^{-1} m^{-3}. Compared with those in the first two stages, the caloric values in the first two stages tend to decrease.

In the fourth stage, the relative content of H_2 was between 3% and 14.95%, with an average of 6.33%. The relative content of N_2 was between 9.8% and 15.61%, with an average of 13.87%. The relative content of CO was between 2.07% and 8.53%, with an average of 4.10%. The relative content of CH_4 was between 0.85% and 2.03%, with an average of 1.13%. The relative content of CO_2 was between 64.73% and 78.33%, with an average of 74.57%. The gas composition is mainly CO_2, and the relative contents of H_2, CO, and CH_4 increase significantly at this stage. This indicates that the combustion area further extends backwards, which is consistent with the analysis in Section 3.1. In addition, the increase in the relative contents of H_2, CO, and CH_4 also indicates that the ability of lignite gasification is significantly enhanced at this stage. The average calorific value of gas production is 1.77 MJ N^{-1} m^{-3} in this stage. The calorific value is significantly greater than that in the second and third stages, which further indicates that the gasification capacity of this stage is enhanced.

In the fifth stage, the relative content of H_2 was between 16.37% and 18.90%, with an average of 17.887%. The relative content of N_2 was between 1.37% and 2.46%, with an average of 1.78%. The relative content of CO was between 8.75% and 23.91%, with an average of 17.88%. The relative content of CH_4 was between 0.50% and 3.06%, with an average of 1.46%. The relative content of CO_2 was between 55.51% and 70.85%, with an average of 61.10%. The relative contents of H_2 and CO rapidly increased at the fifth stage and the end of the fourth stage. An increase in the O_2 concentration accelerates the combustion rate and enhances the efficiency of gasification. Notably, the temperature of T_6 began to increase exponentially when the gasification experiment was carried out for 510 min. This indicates that the combustion process gradually intensified around the T_6 region. Moreover, the degree of backwards extension of the left gasification area is greater than that of the first four stages. At this time, the relative contents of H_2 and CO increased to 18.57% and 16.23%, respectively. In addition, the calorific value of gas production reached its highest value at this stage, with an average value of 5.12 MJ N^{-1} m^{-3}. Under the same

process conditions, the average calorific value obtained in this stage is essentially the same as that of Polish lignite.[2]

3.3.2 Aspen plus process model. Owing to the influence of various factors, physical simulation experiments fail to fully capture the intricacies of lignite gasification. Therefore, this study integrates the Aspen Plus process model to investigate the process of lignite gasification under controlled variable conditions. The gas production of lignite is predicted on the basis of the oxygen enrichment process, ranging from 50% to 100% oxygen concentration. As shown in Fig. 7.

Fig. 7 clearly shows that the oxygen concentration significantly controls the gas production potential of lignite. Specifically, as the oxygen concentration increases, the relative contents of available gases (H_2, CO and CH_4) increase. This observation aligns with both physical simulation experiments and previous studies on lignite gasification.[1,2,39] Notably, the output of effective gas in the physical simulation experiment is relatively lower than that in the Aspen Plus simulation. Two preliminary reasons can be speculated as follows: (1) the Aspen Plus simulation experiment represents an ideal state model where the gasification process is controlled by reactor parameters, eliminating any intermediate losses during gasification; (2) the lignite samples collected from the Chaoyang open-pit coal mine have higher ash yields, resulting in a reduced yield of effective gas components in the physical simulation experiment. Importantly, this study did not gather samples with low ash yields in this region. Consequently, it is unfortunate that this study is unable to quantitatively assess the impact of ash on the gasification efficiency through comparative experiments.

Previous studies on the relative concentration of CO_2 during underground coal gasification have shown some variations. Certain scholars argue that as the oxygen concentration increases in the gasification process, the combustion reaction within the oxidation zone gradually intensifies, leading to an increase in temperature. Consequently, heat transfer to the reduction zone promotes the reduction reaction between CO_2 and C, resulting in an increased yield of CO and a decreased amount of CO_2.[40] An increase in the oxygen concentration is believed by some scholars to increase the reaction rate between oxygen and semicoke, thereby promoting more complete combustion and resulting in an elevated CO_2 content.[41]

The concentration of CO_2 exhibited a pattern of initial increase followed by a decrease in both the physical and numerical simulation data, with its inflection point occurring at 90% of the oxygen concentration. This consistency validates the rationality of the numerical simulation, as described in Section 2.3. A higher concentration of oxygen leads to improved hydrogen production during lignite underground gasification. However, when the oxygen concentration is less than 80% in both simulations, the yields of hydrogen and other effective components remain low. While a higher oxygen concentration enhances the efficiency of producing gases such as hydrogen, it may also result in the complete combustion of semicoke. At an oxygen concentration of 90%, the semicoke reaches a critical value where the ratio of CO to CO_2 is maximized. After the 90% oxygen concentration was reached, the CO_2 production efficiency gradually decreased.

After a 90% concentration in both simulations, the efficiency of CO_2 production decreases with increasing degree of gasification, whereas the efficiency of the active components (H_2, CO, and CH_4) increases. Furthermore, as the degree of gasification progresses, the tar yield tends to increase. When the oxygen concentration reached 90%, the tar yield remained relatively stable. Increasing the gasification intensity has a certain inhibitory effect on tar output. Drawing from the preceding analysis, it can be inferred that at an oxygen concentration of 100%, the lignite gasification process attains a relatively stable state, exhibiting significant potential for gas production and an increased yield of valuable gaseous components. It is evident that a gasification agent with a 100% oxygen concentration is more appropriate for the underground gasification of lignite in Heilongjiang Province.

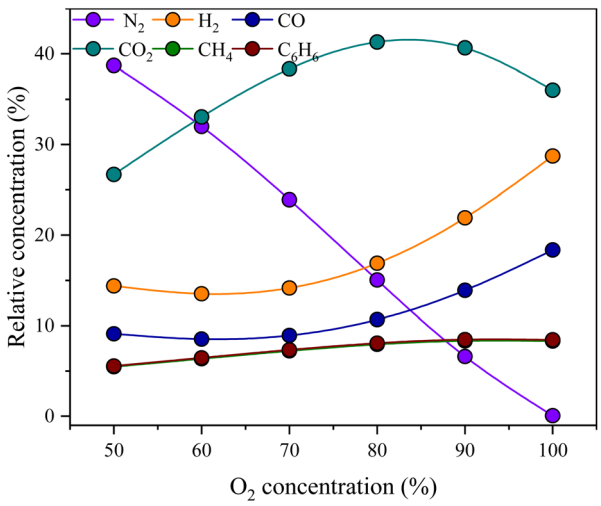

Fig. 7 Changes in the relative product concentration during the oxygen enrichment process.

3.4 Effect of the oxygen concentration on syngas

The oxygen concentration in the gasification agent is one of the key factors for controlling underground gasification.[32] As illustrated in Fig. 5 and 6, at any given stage, when the oxygen concentration remains constant, the temperature, pressure, and concentration of gas products clearly fluctuate. These fluctuations occur at a relatively gradual rate. However, when the gasification reaction stage varies, specifically with changes in the oxygen concentration, the gasification temperature, pressure, and relative concentrations of the gasification products exhibit a stepwise change trend. This finding indicates that the influence of the oxygen concentration on the gasification temperature, pressure, and gasification products is significantly more pronounced than that of the coal used for gasification.

The results of the physical simulation and Aspen Plus process modelling demonstrate that the CO_2 concentration in the syngas tends to increase when the oxygen concentration is 60%, 70%, and 80%. This phenomenon may be attributable to the rapid backwards expansion of the lignite gasification front

depth when the oxygen concentration reaches 80%. Notably, the temperature is approximately 300 °C when a large amount of lignite is gasified in the above three stages. The reaction of coal combustion mainly occurs under these temperature conditions, resulting in a higher relative content of CO_2 in the syngas. This phenomenon has generally been observed in previous studies on lignite.[1,25]

The relative content of CO_2 in the syngas is stable when the oxygen concentration is 90% and decreases when the oxygen concentration is 100%, which may be related to the strong gasification of lignite around the T_6 region. The temperature of a large amount of lignite is above 300 °C at this time, the combustion reaction of lignite has ended, and CO_2 is not produced in large quantities. In contrast, char gradually reacts with oxygen and water to produce CO, H_2 and CH_4. An increase in the oxygen concentration improves the intensity of gasification but also inhibits the generation of CO_2.

Physical simulations show that the relative contents of H_2 and CO in syngas are greater at the beginning of the first stage of gasification, which may be related to the easy combustion and high temperature of lignite near the ignition point. This phenomenon is not found in the Aspen plus process model. Lignite completes H_2 and CO conversion at a faster rate under the action of higher temperatures, which is consistent with the above analysis. With increasing gasification time, the gasification depth and range gradually increased, and the gasification temperature decreased to approximately 300 °C. This leads to an increase in the relative content of CO_2. In addition, in the second and third stages, the relative contents of H_2 and CO are low.

In theory, the gasification process should be continuous, and the temperature should be gradually increased. However, except for the coal near the ignition point, the deep lignite gasified slowly, and the efficiency was low, which may be related to the high ash yield of the experimental lignite. The higher ash yield ($A_d = 26.43\%$ in Table 1) hinders the transfer of gasification to greater depths, which causes the deep coal seam to remain in a low-temperature state for a long time, the relative CO_2 content to increase, and the relative contents of the other components to decrease. Previously reported gasification experiments on low-ash lignite ($A_d = 4.41\%$) were carried out under the same oxygen enrichment process conditions.[27] The relative contents of H_2 and CO reached 30.42% and 26.47%, respectively, when the oxygen concentration was 80%. This result was also reported in previous studies.[6,28] Kashyap *et al.* reported that the volume of H_2, CH_4, and CO in high-ash coal is reduced by 5% compared with that in low-ash coal.[6] The excessive ash yield affects the gasification rate and increases heat loss, which in turn leads to a decrease in the relative contents of H_2 and CO.

When the gasification depth increases, the temperature increases, and the oxygen concentration increases to 80%, 90%, and 100%, the relative contents of H_2 and CO increase gradually. Furthermore, the relative contents of H_2 and CO still increased after the end of the gasification experiment. This shows that the relative content of combustible gas increases with increasing oxygen concentration and gasification temperature, which may be attributed to the significant improvement in the thermodynamic conditions of the gasification reaction.[1] Notably, the relative content of CH_4 was low at all times. This may be related to the release of pressure in the fifth stage. Previous studies have shown that pressure changes can improve the quality of CH_4 and the recovery rate of volatiles in coal seams.[21,24] In the fifth gasification stage, the average relative content of effective components (H_2, CO, and CH_4) is much greater than that in the other stages. This phenomenon is reflected in both the physical simulation and the Aspen Plus process model. This means that the optimal oxygen concentration for underground lignite gasification in Heilongjiang Province is approximately 100%.

4. Conclusions

In this work, the underground gasification potential of lignite in Heilongjiang Province was investigated. The impact of the oxygen enrichment process on the gasification efficiency and product was thoroughly analysed. The main conclusions are summarized below.

(1) Using the physicochemical properties, along with the physical simulation process and pyrolysis data of lignite, a highly reliable Aspen Plus process model was developed. This model is applicable for preliminarily predicting the gasification efficiency of lignite in various regions of Heilongjiang Province.

(2) The concentration of oxygen is the primary determinant influencing gasification efficiency. It modifies the thermodynamic reaction occurring within the gasifier. The transition from lignite combustion reactions to char reactions occurs when the oxygen concentration reaches approximately 90%.

(3) The optimal oxygen concentration for lignite gasification in Heilongjiang Province was determined to be 100%. At this point, the relative concentrations of H_2 and CO reached their maximum values, denoted as 18.90% and 23.91%, respectively. The calorific value reached the highest value of 6.65 MJ N^{-1} m^{-3} at the same time.

Data availability

The authors confirm that the data supporting the findings of this study are available within the article.

Conflicts of interest

There are no conflicts to declare.

Acknowledgements

The authors are sincerely thankful for the financial support of the National Natural Science Foundation of China (No. 42372182; No. 42130802), a project funded by the Priority Academic Program Development of Jiangsu Higher Education Institutions (PAPD), and the Fundamental Research Funds for the Central Universities (2020CXNL11). The authors are sincerely grateful to the Editor, the Real-name Reviewers, and the Anonymous Reviewers for your specific comments on our

manuscript. Your valuable advice and detailed guidance will benefit us greatly in our now and future scientific research work.

References

1 K. Kapusta, M. Wiatowski and K. Stańczyk, An experimental ex-situ study of the suitability of a high moisture ortho-lignite for underground coal gasification (UCG) process, *Fuel*, 2016, **179**, 150–155.

2 K. Stańczyk, A. Smoliński, K. Kapusta, *et al.*, Dynamic experimental simulation of hydrogen oriented underground gasification of lignite, *Fuel*, 2010, **89**(11), 3307–3314.

3 M. Nieć, E. Sermet, J. Chećko, *et al.*, Evaluation of coal resources for underground gasification in Poland. Selection of possible UCG sites, *Fuel*, 2017, **208**, 193–202.

4 L. Feng, D. Maifan, Q. Botao, *et al.*, H_2 production enhancement in underground coal gasification with steam addition: Effect of injection conditions, *Energy*, 2024, **291**, 130379.

5 M. Wiatowski, W. Basa, M. Pankiewicz-Sperka, *et al.*, Experimental study on tar formation during underground coal gasification: Effect of coal rank and gasification pressure on tar yield and chemical composition, *Fuel*, 2024, **357**, 130034.

6 S. Kashyap and P. Vairakannu, Movable injection point–based syngas production in the context of underground coal gasification, *Int. J. Energy Res.*, 2020, **44**(5), 3574–3586.

7 H. Akbarzadeh Kasani and R. J. Chalaturnyk, Coupled reservoir and geomechanical simulation for a deep underground coal gasification project, *J. Nat. Gas Sci. Eng.*, 2017, **37**, 487–501.

8 F. Su, A. Hamanaka, K. Itakura, *et al.*, Evaluation of Coal Combustion Zone and Gas Energy Recovery for Underground Coal Gasification (UCG) Process, *Energy Fuels*, 2017, **31**(1), 154–169.

9 D. Yang, N. Koukouzas, M. Green, *et al.*, Recent development on underground coal gasification and subsequent CO_2 storage, *J. Energy Inst.*, 2016, **89**(4), 469–484.

10 Y. Feng, J. Chen and J. Luo, Life cycle cost analysis of power generation from underground coal gasiffcation with carbon capture and storage (CCS) to measure the economic feasibility, *Resour. Policy*, 2024, **92**, 104996.

11 X. Ren, J. Wu, C. Wang, *et al.*, Research on property and burning behavior of flammable casing for underground coal gasification, *Heliyon*, 2023, **9**(12), e22232.

12 L. Xin, Z. Wang, G. Wang, *et al.*, Technological aspects for underground coal gasification in steeply inclined thin coal seams at Zhongliangshan coal mine in China, *Fuel*, 2017, **191**, 486–494.

13 N. Nakaten, R. Schlüter, R. Azzam, *et al.*, Development of a techno-economic model for dynamic calculation of cost of electricity, energy demand and CO2 emissions of an integrated UCG–CCS process, *Energy*, 2014, **66**, 779–790.

14 Z. Wang, W. Huang, P. Zhang, *et al.*, A contrast study on different gasifying agents of underground coal gasification at Huating Coal Mine, *J. Coal Sci. Eng.*, 2011, **17**(2), 181–186.

15 X. Wang, Q. Zhang and L. Yuan, A coupled thermal-force-chemical-displacement multi-field model for underground coal gasification based on controlled retraction injection point technology and its thermal analysis, *Energy*, 2024, **293**, 130614.

16 H. Zhou, C. Wu, H. Chen, *et al.*, Numerical Simulation of the Temperature Distribution and Evolution Law of Underground Lignite Gasification, *ACS Omega*, 2022, **7**(8), 6885–6899.

17 J. Xie, L. Xin, X. Hu, *et al.*, Technical application of safety and cleaner production technology by underground coal gasification in China, *J. Cleaner Prod.*, 2020, **250**, 119487.

18 B. Xu, L. Chen, B. Xing, *et al.*, Physicochemical properties of Hebi semi-coke from underground coal gasification and its adsorption for phenol, *Process Saf. Environ. Prot.*, 2017, **107**, 147–152.

19 G. Perkins, Underground coal gasification–Part I: Field demonstrations and process performance, *Prog. Energy Combust. Sci.*, 2018, **67**, 158–187.

20 Y. M. Alshammari and K. Hellgardt, A new HYSYS model for underground gasification of hydrocarbons under hydrothermal conditions, *Int. J. Hydrogen Energy*, 2014, **39**(24), 12648–12656.

21 R. Mandal and T. Maity, Operational process parameters of underground coal gasification technique and its control, *J. Process Control*, 2023, **129**, 103031.

22 M. Wiatowski, K. Kapusta and R. Muzyka, Study of properties of tar obtained from underground coal gasification trials, *Fuel*, 2018, **228**, 206–214.

23 W. Gao, R. Zagorščak and H. R. Thomas, Insights into solid-gas conversion and cavity growth during Underground Coal Gasification (UCG) through Thermo-Hydraulic-Chemical (THC) modelling, *Int. J. Coal Geol.*, 2021, **237**, 103711.

24 K. Kapusta, M. Wiatowski, H. R. Thomas, *et al.*, Experimental simulations of methane-oriented underground coal gasification using hydrogen - The effect of coal rank and gasification pressure on the hydrogasification process, *Int. J. Hydrogen Energy*, 2023, **48**(3), 921–932.

25 M. Laciak, K. Kostúr, M. Durdán, *et al.*, The analysis of the underground coal gasification in experimental equipment, *Energy*, 2016, **114**, 332–343.

26 S. K. De and V. Prabu, Experimental studies on humidified/water influx O_2 gasification for enhanced hydrogen production in the context of underground coal gasification, *Int. J. Hydrogen Energy*, 2017, **42**(20), 14089–14102.

27 J. Zhao, H. Liu, X. Pan, *et al.*, Study on O_2/CO_2 underground coal gasification effect with different oxygen-enriched conditions, *Coal Sci. Technol.*, 2017, **45**(06), 214–220.

28 A. Arabkhalaj, H. Ghassemi and M. R. Shahsavan, Thermodynamic evaluation of integrated gasification combined cycle: Comparison between high-ash and low-ash coals, *Int. J. Energy Res.*, 2016, **40**(12), 1638–1651.

29 R. Zagorščak, S. Sadasivam, H. R. Thomas, *et al.*, Experimental study of underground coal gasification (UCG)

of a high-rank coal using atmospheric and high-pressure conditions in an ex-situ reactor, *Fuel*, 2020, **270**, 117490.

30 K. Stańczyk, K. Kapusta, M. Wiatowski, *et al.*, Experimental simulation of hard coal underground gasification for hydrogen production, *Fuel*, 2012, **91**(1), 40–50.

31 M. Wiatowski, K. Stańczyk, J. Świądrowski, *et al.*, Semi-technical underground coal gasification (UCG) using the shaft method in Experimental Mine "Barbara", *Fuel*, 2012, **99**, 170–179.

32 H. Liu, S. Liu, F. Chen, *et al.*, Mathematical Modeling of the Underground Coal Gasification Process in One Gasification Cycle, *Energy Fuels*, 2019, **33**(2), 979–989.

33 E. Andrianopoulos, A. Korre and S. Durucan, Chemical Process Modelling of Underground Coal Gasification and Evaluation of Produced Gas Quality for End Use, *Energy Procedia*, 2015, **76**, 444–453.

34 K. Kapusta, Effect of Lignite Properties on Its Suitability for the Implementation of Underground Coal Gasification (UCG) in Selected Deposits, *Energies*, 2021, **14**(18), 5816.

35 K. Kostúr and T. Sasvári, Research of underground gasification lignite, *Acta Montan. Slovaca*, 2010, **15**(2), 121–133.

36 Y. Liu, Y. Jiang, S. Deng, *et al.*, Review of coal gasification process simulation based on Aspen Plus software, *Henan Chem. Ind.*, 2010, **27**(14), 25–28.

37 W. Wang, Y. Sang and J. Wu, The Lignite Coal Pyrolysis Process Simulation Based on Aspen Plus, *Chem. Ind. Eng.*, 2011, **28**(3), 49–53.

38 He Zhou, *Main Controlling Factors and Gas Production Potential Evaluation of Geological Selection Area of Underground Coal Gasification – A Case Study of Songhe Minefield in Western Guizhou*, China University of Mining and Technology, Xuzhou, 2022.

39 M. Gur, N. Eskin, H. Okutan, *et al.*, Experimental results of underground coal gasification of Turkish lignite in an ex-situ reactor, *Fuel*, 2017, **203**, 997–1006.

40 S. Zhang, G. Chen, M. Dong, *et al.*, Steam Gasification Law of Youyuyuanbao Coal Char, *Coal Technol.*, 2014, **33**(9), 255–258.

41 W. Huang, *Study on Comprehensive Evaluation and Stable Production Technology for Underground Gasification of Residual Coal*, China University of Mining and Technology, Xuzhou, 2014.